Electronic Supporting Information (ESI)

Bismuth-based electrocatalytic scheme enabling efficient and selective electrosynthesis of 4-aminophenol in acidic media

Fitri Nur Indah Sari[a], Cheng-Yi Su[a], Shih-Ching Huang[a], and Chia-Yu Lin[a, b, c*]

[b]*Department of Chemical Engineering, National Cheng Kung University, Tainan City 70101, Taiwan*
[c]*Hierarchical Green-Energy Materials (Hi-GEM) Research Center, National Cheng Kung University, Tainan 70101, Taiwan.*
[d]*Program on Key Materials & Program on Smart and Sustainable Manufacturing, Academy of Innovative Semiconductor and Sustainable Manufacturing, National Cheng Kung University, Tainan 70101 Taiwan*

* Corresponding author: cyl44@mail.ncku.edu.tw (Prof. Chia-Yu Lin)

Contents

Experimental

Chemicals and materials. All the chemicals, including acetone (99%, Echo Chemical), $Bi(NO_3)_3.5H_2O$ (98%, Sigma-Aldrich), ethanol (95%, Echo Chemical), H_2SO_4 (97%; J.T. Baker), HNO_3 (70%, Sigma-Aldrich), 4-nitrophenol (4-NP; 99%, Alfa Aesar), HCl (37%, Riedel-de Haen), 4-aminophenol (4-AP; 98%, Alfa Aesar) were used as received. Deionized water (18.2 MΩ cm; DIW) was used for the electrode cleaning and preparation of electrolyte solution throughout the work. Copper foil (thickness: 0.1 mm; ≥99.99%; Central Research Company, Taiwan), Ti foil (thickness: 0.25 mm; 99.7%; Sigma-Aldrich), and Toray carbon paper (TGP-H-60, Thermo Fisher Scientific) were used as the electrode substrate. The copper foil was successively cleaned with acetone for 10 min and diluted HCl aqueous solution (~1.9%) for 10 min under sonication before its usage. The Ti foil was successively cleaned with ethanol for 10 min and DIW for 10 min under sonication before its usage. The Toray carbon paper was successively cleaned with nitric acid for 5 min, ethanol for 5 min, and DIW for 10 min under sonication before its usage.

Electrochemical preparation of the bismuth film modified electrode. The bismuth film modified copper electrode, designated as $Cu|Bi_{film}$, was prepared by electrodeposition in the plating solution containing nitric acid (1.0 M) and bismuth nitrate (30 mM) at -5 mA cm^{-2} for 300 s using an Iviumn-Stat workstation (Ivium Technologies B.V., Netherlands) connected with a customized three-electrode single-compartment electrochemical cell with Ag/AgCl (sat'd KCl) reference electrode and Pt foil (1 cm × 4 cm) counter electrode.

Electrochemical characterization. The behaviour of the electrocatalytic reduction of 4-NP (*e*-NPR) at different electrode substrates was investigated using an Iviumn-Stat workstation (Ivium Technologies B.V., Netherlands) connected with a well-sealed customized two-compartment H-cell. The anodic compartment and cathodic compartment of the H-cell were separated with a Nafion® 117 film. The copper foil, carbon paper, or Ti foil was used as the working electrode (geometric area: 1.2 cm^{-2}) and placed with a Ag/AgCl reference electrode in the cathodic compartment, whereas the Pt counter electrode was placed in the anodic compartment. Unless otherwise noted, the H_2SO_4 solution containing 4-AP (10 mM) and Bi ions (25 ppm) was used as the electrolyte solution and deaerated under N_2 purge for 30 min prior to the electrochemical characterization. All the potentials were 95% iR compensated and reported against the reversible hydrogen electrode (RHE) scale using Eq. (1):

$$E\ (V\ vs.\ RHE) = E\ (V\ vs.\ Ag/AgCl) + 0.197 + 0.059 \times pH \qquad (1)$$

The *e*-NPR at different electrode substrates was examined using cyclic voltammetry (CV) at a scan rate of 10 mV s^{-1} and 4-h controlled-potential electrolysis (CPE). The conversion of 4-NP (χ_{NP}) after each CPE was determined by the method reported previously.[1, 2] Briefly, 0.05 mL catholyte was alkalized with 7.45 mL NaOH solution (0.5 M) and then subjected to UV-vis measurement with an Agilent Cary® 60 UV-Vis spectrophotometer. Thereafter, the measured absorbance at λ = 400 nm was converted to the 4-NP concentration (C_{NP}) using a pre-determined calibration curve, and then the obtained C_{NP} value was used to determine χ_{NP} using Eq. (2) and known initial 4-NP concentration ($C_{NP,0}$= 10.0 mM).

$$\chi_{NP}\ (\%) = \frac{C_{NP,0} - C_{NP}}{C_{NP,0}} \times 100\% \qquad (2)$$

The amount of 4-AP generated from each CPE (N_{AP}) was quantified using a Shimadzu Nexera-I LC-2040C 3D high-performance liquid chromatography (HPLC) system equipped with a Shodex HILICpak VG-50 4E column and a photodiode array detector (PDA; λ = 233 nm). Methanol-water solution (volume ratio: 3:7) was used as eluent for HPLC analyses at a flow rate of 0.6 mL min^{-1} at 40 °C. The HPLC signal for the formation of 4-AP was confirmed using the ultra-high performance liquid chromatography-tandem with mass spectrometry in our previous work.[1] N_{AP} was obtained by converting the measured HPLC signals with routinely updated calibration curves The Faradaic efficiency (FE_{AP}) and selectivity (S_{AP}) for 4-AP production were determined using Eq. 3 and Eq. 4, respectively.

$$FE_{AP}\ (\%) = \frac{N_{AP} \times 6F}{Q_{total}} \times 100\% \quad (3)$$

$$S_{AP}\ (\%) = \frac{N_{AP}}{V_{catholyte} \times (C_{NP,0} - C_{NP})} \times 100\% \quad (4)$$

where F is Faradaic constant (96,485 C mol^{-1}), Q_{total} is the total charge passage, and $V_{catholyte}$ is the volume of the catholyte.

Physical characterization. X-ray diffraction (XRD) analyses were performed with a Bruker D8 DISCOVER X-ray diffractometer. The surface morphology of the electrode substrates after CPEs was characterized using a Hitachi SU-8010 scanning electron microscope (SEM).

Table S1 Comparison on the electrocatalytic performance of the developed Bi^{3+}/Bi^0-based *e*-NPR system[a] with those reported previously.

Catalytic material	E (V vs. RHE)	Electrolyte	χ_{NP} (%)	FE_{AP} (%)	S_{AP} (%)	R_{AP} (μmole cm^{-2} h^{-1})	Ref.
CP|*micro*NiFeP (r= 0.5)	0.0	0.5 M phosphate buffer containing 4 mM 4-NP	37.7 ± 1.1[b]	95.3 ± 1.7[b]	96.2 ± 1.1[b]	13.3 ± 0.3[b]	1
CP|*micro*NiFeP (r= 0.5)	0.1	0.5 M phosphate buffer containing 4 mM 4-NP	3.5 ± 0.5[b]	64.7 ± 2.8[b]	48.8 ± 1.9 [b]	0.6 ± 0.1[b]	1
$Cu(OH)_2$ nanorods decorated Cu foam	~0.02	1.0 M KOH containing 10 mM 4-NP and 0.1 M $NaBH_4$	~100	96.8	N.A.[c]	~250	3
TiO_2 with exposed [001] facets and oxygen vacancy	-0.66	0.1 M Na_2SO_4 (pH 5) containing 0.1 mM 4-NP	99.3	N.A.[c]	~87	~0.22	4
Porous Au micropillars	~ -0.05	0.4 M Na_2SO_4 (pH 2) containing 5 mM 4-NP	~99	N.A.[c]	~100	N.A.[c]	5
Superhydrophilic Ru-phytic acid/nickel foam	~ -0.67	1.0 M KOH containing 5.0 mM 4-NP	94.7	73.2	99.0	15.6	6
$CuCo_2O_4$/nickel foam	~ -0.20	1.0 M KOH containing 20 mM 4-NP	95.8	89	97.2	~14.03	7
Carbon black supported Mn-MIL-100 framework	~-0.485	0.25 M NaCl (pH 2) containing 0.7 mM 4-NP	96[d]	76[d]	N.A.[c]	N.A.[c]	8
Pt nanoparticles	-0.023	0.5 M H_2SO_4 containing 33.2 μM 4-NP	61.5[e]	14.7[e]	N.A.[b]	N.A.[b]	9
Ag/Ni-MOF/nickel foam	~ 0.024	1.0 M KOH containing 25 mM 4-NP	98.4[e]	99.8[e]	N.A.[b]	~197[e]	10
Bi^{3+}/Bi^0 redox species	0.1	0.5 M H_2SO_4 containing 10 mM 4-NP and 25 ppm Bi^{3+}	73.8 ± 1.0[e]	90.1 ± 3.5[e]	100.32 ± 3.2[e]	46.9 ± 2.3[e]	This work

[a]: with copper foil as the electrode substrate; [b]: Based on 4-h electrolysis; [c]:Data not available; [d]: Based on 12-h electrolysis; [e]: based on 5-h electrolysis;

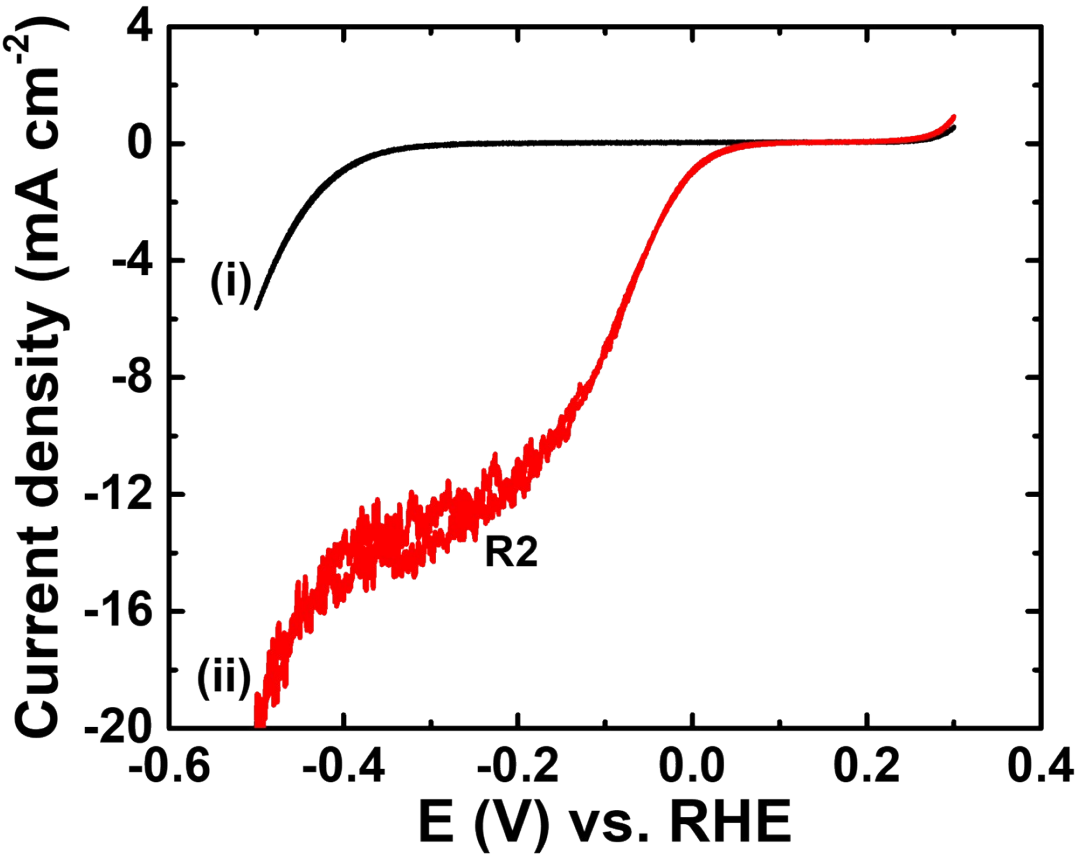

Figure S1 CVs of the copper foil recorded at a scan rate of 10 mV s^{-1} in the H_2SO_4 solution (0.5 M) containing 4-NP of different concentrations (i: 0 mM; ii: 10 mM). The cathodic wave R2 was associated with *e*-NPR.

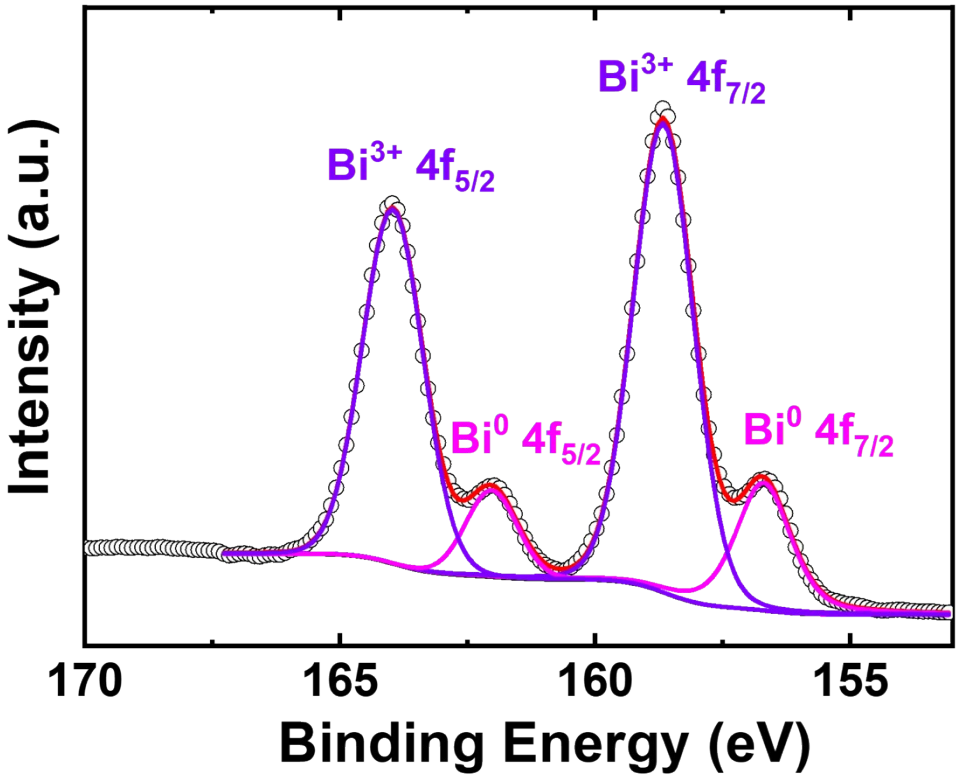

Figure S2 Bi 4f XPS spectrum of copper foil obtained after 4-h CPE at 0.15 V vs. RHE. The presence of Bi^{3+} is attributed to the oxidation of Bi^0 upon exposure air.

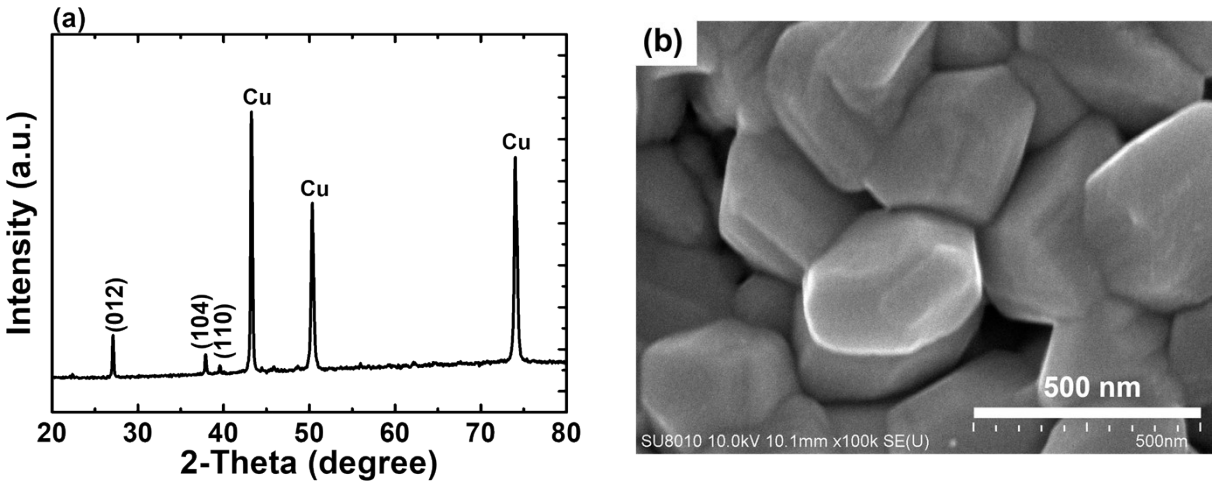

Figure S3 (a) XRD pattern and (b) SEM image of the Cu|Bi_{film} electrode.

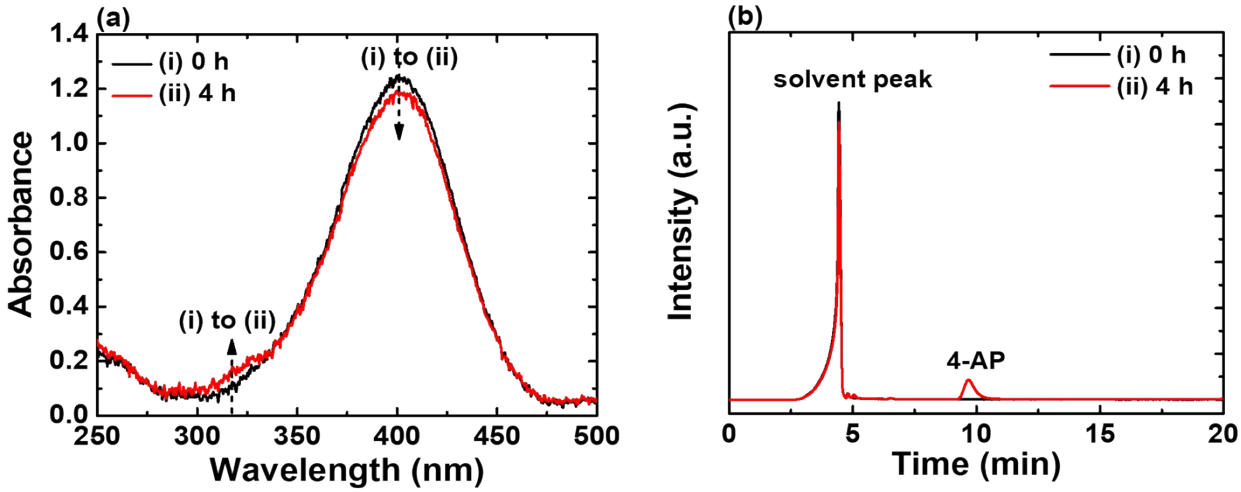

Figure S4 (a) UV-vis spectra and (b) HPLC spectra of the 4-NP (10 mM)-containing H_2SO_4 solution before and after the 4-h incubation of the Cu|Bi_{film} electrode without applying any electricity.

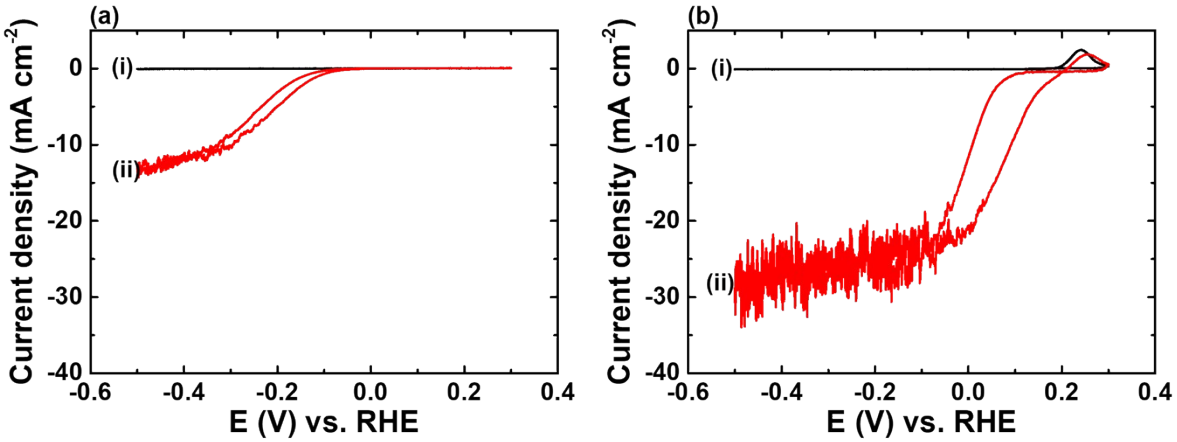

Figure S5 CVs of the carbon paper in (a) the H_2SO_4 solution (0.5 M) containing 4-NP of different concentrations (i: 0 mM; ii: 10 mM), and (b) the H_2SO_4 solution (0.5 M) containing Bi^{3+} ions (25 ppm) and 4-NP of different concentrations (i: 0 mM; ii: 10 mM).

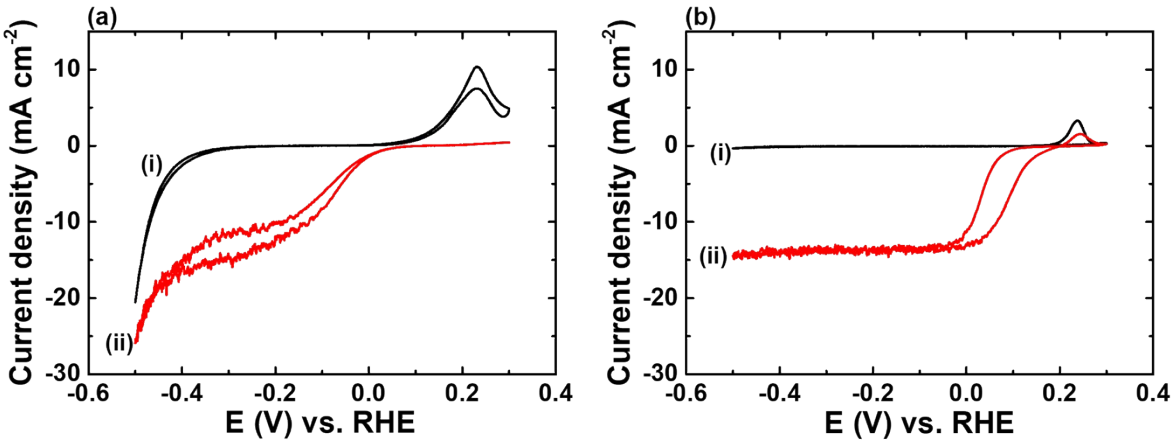

Figure S6 CVs of the Ti foil in (a) the H_2SO_4 solution (0.5 M) containing 4-NP of different concentrations (i: 0 mM; ii: 10 mM), and (b) the H_2SO_4 solution (0.5 M) containing Bi^{3+} ions (25 ppm) and 4-NP of different concentrations (i: 0 mM; ii: 10 mM).

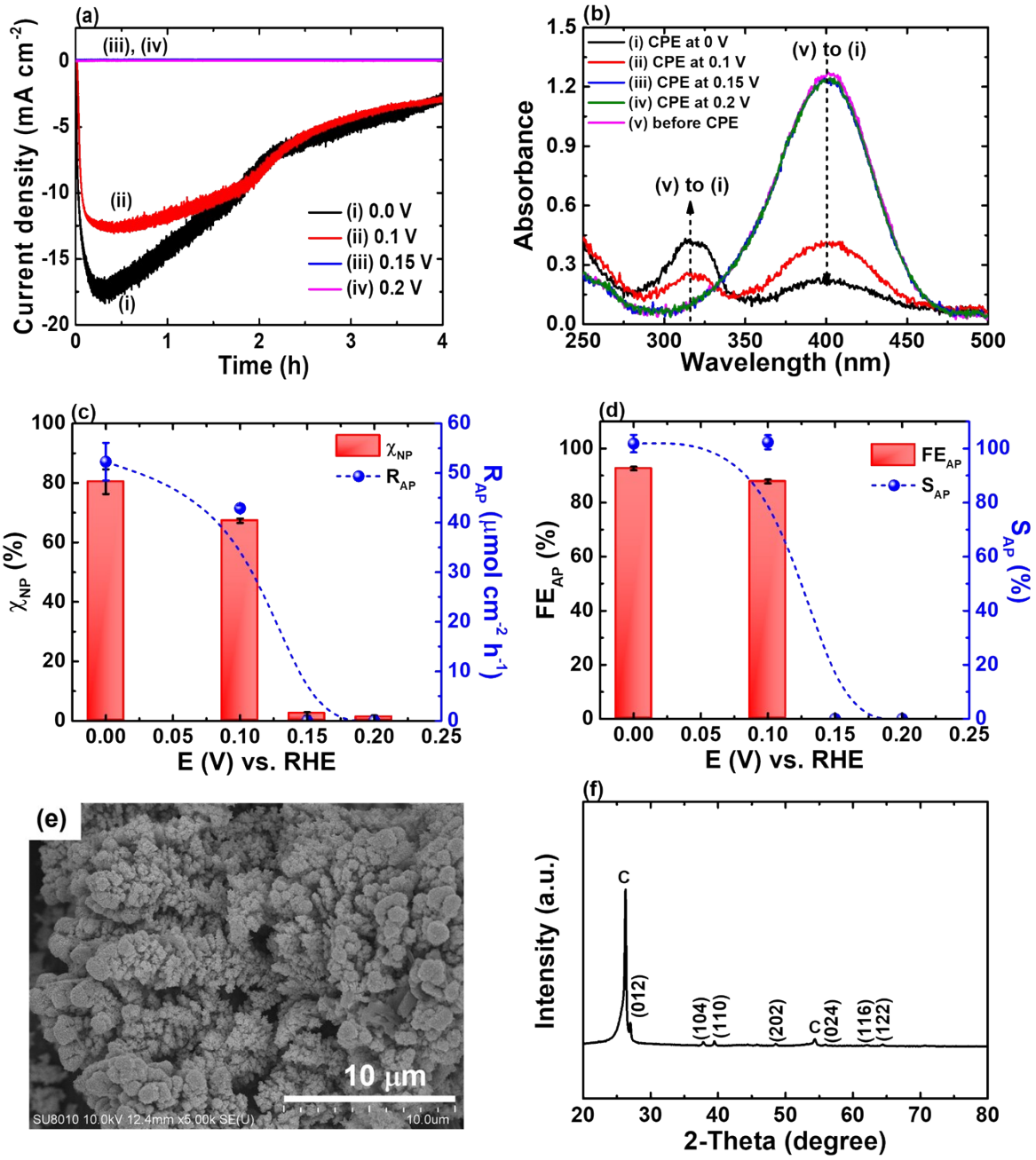

Figure S7 (a) Current transients, (b) UV-vis spectra, (c) χ_{NP} and R_{AP}, and (d) FE_{AP} and S_{AP} obtained from the 4-h CPEs using the carbon paper as electrode substrate at various applied potentials. (e) SEM image and (f) XRD pattern of the carbon paper obtained after 4-h CPE at 0.0 V vs. RHE. All CPEs were performed in the deaerated H_2SO_4 solution (0.5 M) containing 4-NP (10 mM) and Bi^{3+} ions (25 ppm).

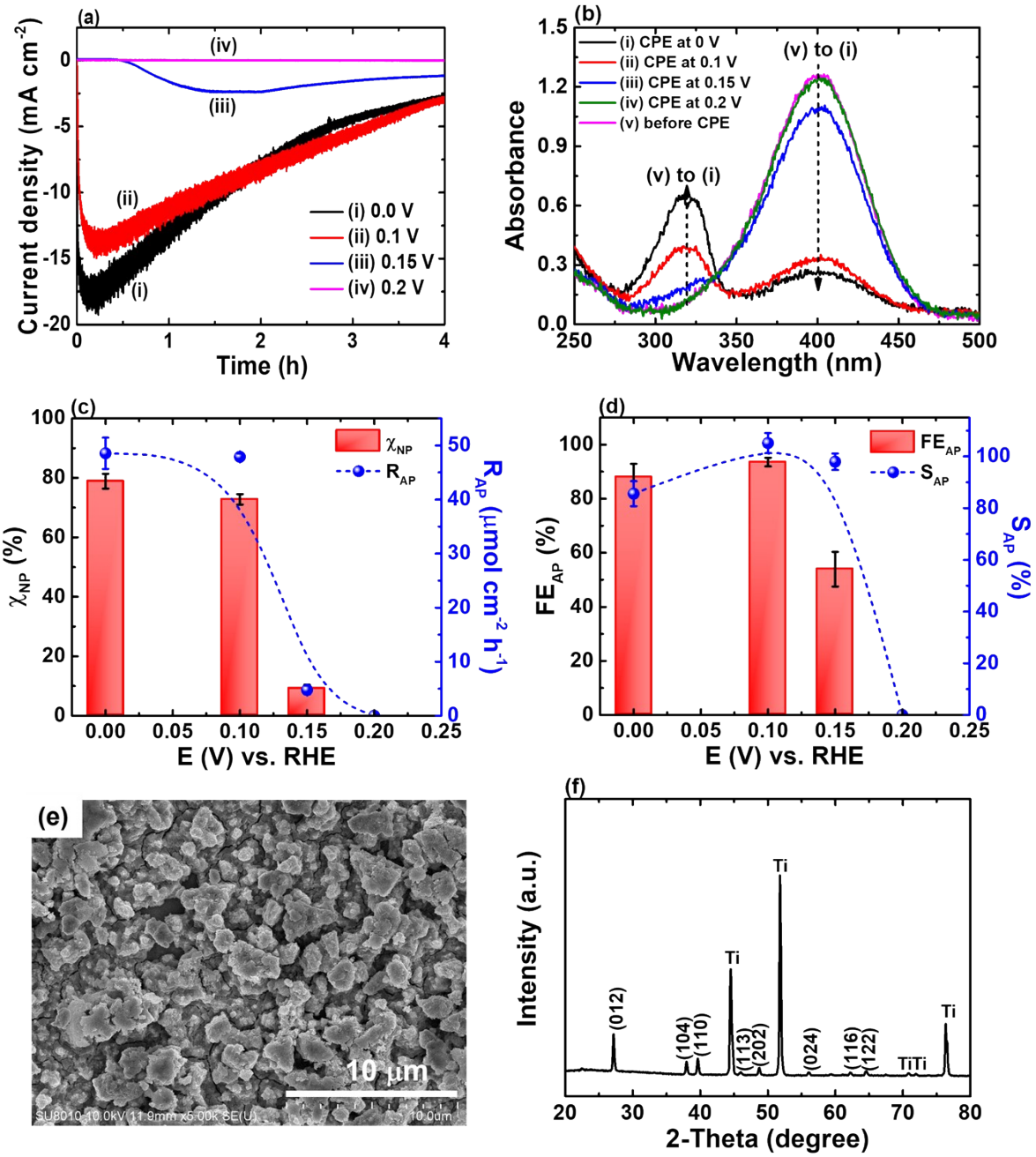

Figure S8 (a) Current transients, (b) UV-vis spectra, (c) χ_{NP} and R_{AP}, and (d) FE_{AP} and S_{AP} obtained from the 4-h CPEs using the Ti foil as electrode substrate at various applied potentials. (e) SEM image and (f) XRD pattern of the Ti foil obtained after 4-h CPE at 0.0 V vs. RHE. All CPEs were performed in the deaerated H_2SO_4 solution (0.5 M) containing 4-NP (10 mM) and Bi^{3+} ions (25 ppm).

References

1. P. S. Ong, S.-C. Huang, C.-Y. Lin and N. Lerkkasemsan, *Mater. Today Sustain.*, 2023, **24**, 100547.
2. S.-C. Huang, Z.-X. You, S.-M. Jhang and C.-Y. Lin, *J. Environ. Chem. Eng.*, 2022, **10**, 108882.
3. X. Pang, H. Bai, H. Zhao, W. Fan and W. Shi, *ACS Catal.* 2022, **12**, 1545-1557.
4. C. C. Ni, Y. F. Li, X. Z. Meng, S. L. Liu, S. Y. Luo, J. Guan and B. Jiang, *Chem. Eng. J.* 2021, **411**, 128485.
5. M. Tranchant, A. Serra, C. Gunderson, E. Bertero, J. Garcia-Amoros, E. Gomez, J. Michler and L. Philippe, *Appl. Catal. A-Gen.*, 2020, **602**, 117698.
6. M. Liu, A. Kong, J. Zhang, Y. Fu and W. Li, *Int. J. Hydrog. Energy*, 2022, **47**, 2187-2199.
7. T. Wu, X. Huang, H. L. Zhang, Z. D. Wei, M. Wang, *ACS Catal.*, 2022, **12**, 58-65
8. D. Chen, Y. Zhang, P. Mao, X. Jiang, J. Li, A. Sun and J. Shen, *J. Electroanal. Chem.*, 2021, **903**, 115824.
9. T. X. Wu, G. Z. Wang, Y. X. Zhang, S. H. Kang and H. M. Zhang, *New J. Chem.*, 2017, **41**, 7012-7019.
10. H. Zhao, X. Pang, Y. Huang, Y. Bai, J. Ding, H. Bai and W. Fan, *Chem. Commun.*, 2022, **58**, 13499-13502.